British Journal of Pharmacology

British Journal of Pharmacology (2018) **175** 4167–4182 4167

RESEARCH PAPER

Successful treatment of established heart failure in mice with recombinant HDL (Milano)

Correspondence Bart De Geest, Centre for Molecular and Vascular Biology, Department of Cardiovascular Sciences, Catholic University of Leuven, Campus Gasthuisberg, Herestraat 49 bus 911, Leuven 3000, Belgium. E-mail: bart.degeest@kuleuven.be

Received 14 November 2017; **Revised** 9 July 2018; **Accepted** 12 July 2018

Joseph Pierre Aboumsallem[1,*], Mudit Mishra[1,*], Ruhul Amin[1], Ilayaraja Muthuramu[1], Herman Kempen[2] and Bart De Geest[1]

[1]Centre for Molecular and Vascular Biology, Department of Cardiovascular Sciences, Catholic University of Leuven, Leuven, Belgium, and [2]The Medicines Company (Schweiz) GmbH, Zürich, Switzerland

*Both authors contributed equally to this study.

BACKGROUND AND PURPOSE

The pleiotropic properties of HDL may exert beneficial effects on the myocardium. The effect of recombinant HDL_{Milano} on established heart failure was evaluated in C57BL/6 mice.

EXPERIMENTAL APPROACH

Mice were subjected to transverse aortic constriction (TAC) or sham operation at the age of 14 weeks. Eight weeks later, TAC and sham mice were each randomized into three different groups. Reference groups were killed at day 56 after the operation for baseline analysis. Five i.p. injections of recombinant HDL_{Milano} (MDCO-216), 100 $mg \cdot kg^{-1}$, or an equivalent volume of control buffer were administered with a 48 h interval starting at day 56. Endpoint analyses in the control buffer groups and in the MDCO-216 groups were executed at day 65.

KEY RESULTS

Lung weight in MDCO-216 TAC mice was 25.3% lower than in reference TAC mice and 27.9% lower than in control buffer TAC mice and was similar in MDCO-216 sham mice. MDCO-216 significantly decreased interstitial fibrosis and increased relative vascularity compared to reference TAC mice and control buffer TAC mice. The peak rate of isovolumetric relaxation in MDCO-216 TAC mice was 30.4 and 36.3% higher than in reference TAC mice and control buffer TAC mice respectively. Nitro-oxidative stress and myocardial apoptosis were significantly reduced in MDCO-216 TAC mice compared to control buffer TAC mice.

CONCLUSIONS AND IMPLICATIONS

MDCO-216 improves diastolic function, induces regression of interstitial fibrosis and normalizes lung weight in mice with established heart failure. Recombinant HDL may emerge as a treatment modality in heart failure.

Abbreviations

AAV8-A-I, adeno-associated viral serotype 8-human apo A-I; apo, apolipoprotein; LV, left ventricle; POPC, 1-palmitoyl-2-oleoyl-sn-glycero-3-phosphatidylcholine; TAC, transverse aortic constriction

DOI:10.1111/bph.14463

Introduction

Heart failure is the cardiovascular epidemic of the 21st century (Luscher, 2015). Epidemiological studies support an independent inverse association between HDL cholesterol levels and heart failure incidence. In the Framingham Heart Study participants free of coronary heart disease at baseline, decreased HDL cholesterol levels were independently associated with heart failure incidence after adjustment for interim myocardial infarction and clinical covariates (Velagaleti *et al.,* 2009). Low HDL cholesterol levels and low levels of apolipoprotein (apo) A-I carry an unfavourable prognosis in patients with heart failure independent of the aetiology (Iwaoka *et al.,* 2007; Mehra *et al.,* 2009).

The pleiotropic properties of HDL may exert beneficial effects on the myocardium (Shah *et al.,* 2013; Gordts *et al.,* 2014; Van Linthout *et al.,* 2015; Muthuramu *et al.,* 2017). We have recently shown that selective adeno-associated viral serotype 8-human *apo A-I* (AAV8-A-I) HDL-raising gene therapy improves cardiac function both in the absence and in the presence of pressure overload and counteracts adverse ventricular remodelling in mice with pressure overload, as shown by reduced myocardial fibrosis, an increased capillary myocardial density, and reduced apoptosis in the myocardium (Amin *et al.,* 2017). HDL has been shown to down-regulate the **angiotensin II type 1 (AT_1) receptor** (Van Linthout *et al.,* 2009; Lin *et al.,* 2011; Alexander *et al.,* 2017a). Furthermore, HDL inhibits mechanical stress-induced autophagy and hypertrophy in cultured cardiomyocytes (Lin *et al.,* 2015). Continuous infusion of HDL has been shown to inhibit cardiac hypertrophy *in vivo* (Lin *et al.,* 2011; Lin *et al.,* 2015), which may be mediated at least in part *via* down-regulation of the AT_1 receptor. Selective HDL-raising gene therapy also exerted anti-hypertrophic effects on the myocardium under conditions of pressure overload (Amin *et al.,* 2017). However, all these studies are not the equivalent of a clinical intervention in patients with established disease since treatment is initiated before the onset of disease.

Apo A-I_{Milano} is an apo A-I mutant resulting from an arginine 173 to cysteine mutation and was described in 1980 in a family from Limone sul Garda in Northern Italy (Franceschini *et al.,* 1980; Weisgraber *et al.,* 1980). Heterozygous carriers of the apo A-I_{Milano} mutant in this family are characterized by apparent longevity (Gualandri *et al.,* 1985) and much less atherosclerosis than expected based on their plasma levels of HDL cholesterol [in the lowest 5th percentile (100–300 $mg \cdot L^{-1}$)] (Sirtori *et al.,* 2001). MDCO-216 is a form of reconstituted HDL that consists of a complex of highly purified recombinant dimeric apoA-I_{Milano} and POPC and has previously been studied as a predecessor compound ETC-216 (Kallend *et al.,* 2016). The safety of MDCO-216 has been established in clinical studies (Kallend *et al.,* 2016; Kempen *et al.,* 2016a; Kempen *et al.,* 2016b; Reijers *et al.,* 2017).

The objective of the current study was to demonstrate the efficacy of an HDL-targeted intervention on established non-ischaemic heart failure in an experimental animal model. Therefore, we studied the effect of administration of apo A-I_{Milano}/phospholipid complexes on established heart failure induced by transverse aortic constriction (TAC) in C57BL/6 mice 56 days before intervention. TAC is a commonly used model for pressure overload-induced cardiac hypertrophy and heart failure (Qin *et al.,* 2015). TAC initially leads to compensatory hypertrophy of the heart, but over time, the response to chronic haemodynamic overload becomes maladaptive and results in cardiac dilatation and heart failure.

Methods

Recombinant HDL_{Milano}

MDCO-216 is a 1:1 by weight complex of recombinant dimeric apo A-I_{Milano} and POPC. It was provided by The Medicines Company (Parsipanny, NJ, USA) as a solution in buffer containing mannitol 43.6 mM, sucrose 181 mM, $NaH_2PO_4 \cdot 2H_2O$ 3.46 mM and $Na_2HPO_4 \cdot 7H_2O$ 8.43 mM.

In vivo experiments evaluating the effect of MDCO-216 on established heart failure in mice

All experimental procedures in animals were performed in accordance with protocols approved by the Institutional Animal Care and Research Advisory Committee of the Catholic University of Leuven (Approval number: P154/2013). Animal studies are reported in compliance with the ARRIVE guidelines (Kilkenny *et al.*, 2010; McGrath and Lilley, 2015). Mice were housed in filter top type II cages containing five mice or less in the semi-specific pathogen-free facility of KU Leuven at Gasthuisberg. A semi-natural 12 h cycle of light and dark was maintained, and temperature was kept in a range from 21 to 22°C. C57BL/6NTac mice, originally obtained from Taconic (Ry, Denmark), were locally bred in the animal unit at Gasthuisberg and were fed standard chow diet (Sniff Spezialdiäten GMBH, Soest, Germany). Anaesthesia and sham and TAC operations were performed in the same animal unit where the mice were born and housed. Following recovery, mice were returned to their original cages and monitored daily until the end of the experiment.

To induce pressure overload, the TAC procedure was executed as described before (Muthuramu *et al.,* 2017b). Briefly, anaesthesia was induced with a single i.p. injection of sodium pentobarbital (Nembutal®, Ceva Sante Animale, Brussels, Belgium) at a dose of 40–70 $mg \cdot kg^{-1}$ body weight. Mice were put in the supine position, and temperature was maintained at 37°C with a heating pad. A horizontal skin incision of 0.5 to 1 cm in length was made at the level of the suprasternal notch. A 2 to 3 mm longitudinal cut was performed in the proximal portion of the sternum, and the thymus gland was retracted. This allowed visualization of the aortic arch under low-power magnification. A wire with a snare at the end was passed under the aorta between the origin of the right innominate artery and the left common carotid artery. A 7–0 silk suture (Ethicon, Johnson & Johnson, Livingston, Scotland, UK) was snared with the wire and pulled back around the aorta. Subsequently, a bent 27-gauge needle (BD Microlance®, BD, Franklin Lakes, NJ, USA) was placed next to the aortic arch, and the suture was snugly tied around the needle and the aorta. Afterwards, the needle was quickly removed. The skin was closed, and mice were allowed to recover on a warming pad until they were fully awake. The sham procedure was

identical except that no constriction on the aortic arch was applied. Postoperative analgesia was applied immediately following the sham or TAC intervention. Specifically, buprenorphine (Temgesic®) (Reckitt Benckiser Healthcare Ltd., Hull, UK) was administered at a dose of 0.1 mg·kg^{-1} body weight s.c. for postoperative pain relief. Mice were killed at the end of the experiment by an i.p. injection of sodium pentobarbital (200 mg·kg^{-1}) and cervical dislocation.

Study design

The study design is illustrated in Figure 1. Sham or TAC surgery was performed at the age of 14 weeks in male mice. Group assignment in the sham and TAC arm of the study at day 56 after operation was performed at random. To determine cardiac structure and function and the degree of established heart failure at baseline prior to MDCO-216 administration, endpoint analyses in the reference group were performed at day 56. Sham and TAC intervention groups were treated with five i.p. injections of 100 mg·kg^{-1} (protein concentration) of MDCO-216 (protein concentration product 15 mg·mL^{-1}), at an interval of 48 h each starting at day 56 after the operation. Control buffer mice were injected with the same volume of the buffer solution pH 7.4 containing mannitol 43.6 mM, sucrose 181 mM, $NaH_2PO_4{\cdot}2H_2O$ 3.46 mM and $Na_2HPO_4{\cdot}7H_2O$ 8.43 mM (Figure 1). Endpoint analyses in the sham and TAC MDCO-216 and control buffer groups were performed at day 65. In the first experimental level, mice were assigned for haemodynamic quantification and morphometric and histological analysis. The second experimental level consisted of mice that did not undergo perfusion fixation and that were used for quantification of tissue and organ weights and for quantification of protein and mRNA levels. Primary outcomes were the effect of MDCO-216 on lung weight and on cardiac functional parameters in TAC mice. Secondary outcomes were histological and morphometric parameters of cardiac structure in TAC mice. All outcomes were pre-specified before the onset of the study.

In vivo haemodynamic measurements

Invasive haemodynamic measurements were performed 56 or 65 days after TAC or after sham operation as described previously (Muthuramu *et al.,* 2017b). Mice were anaesthetized by i.p. administration of 1.4 g·kg^{-1} urethane (Sigma-Aldrich, Steinheim, Germany). Body temperature was maintained with a heating pad and monitored with a rectal probe. An incision in the right carotid artery was made with a 26-gauge needle between a distal and proximal non-occlusive ligation of the artery. A 1.0 French Millar pressure catheter (SPR-67/NR; Millar instruments, Houston, TX, USA) was inserted and advanced to the left ventricle (LV). After stabilization of the catheter, heart rate, maximal systolic LV pressure, minimal diastolic LV pressure, the peak rate of isovolumetric LV contraction (dP/dt_{max}) and the peak rate of isovolumetric LV relaxation (dP/dt_{min}) were measured. The end-diastolic LV pressure was calculated manually from the pressure in function of time curves. The time constant of isovolumetric LV pressure fall, τ, was calculated following the method of Weiss (τ-Weiss) and the method of Glantz (τ-Glantz) using LabChart software version 8 (ADInstruments, Oxford, UK). Arterial blood pressure measurements were obtained after withdrawal of the catheter from the LV to the ascending aorta. Data were registered with a Powerlab Bridge Amplifier and Chart Software (sampling rate 2000 Hz; ADInstruments Ltd, Oxford, UK).

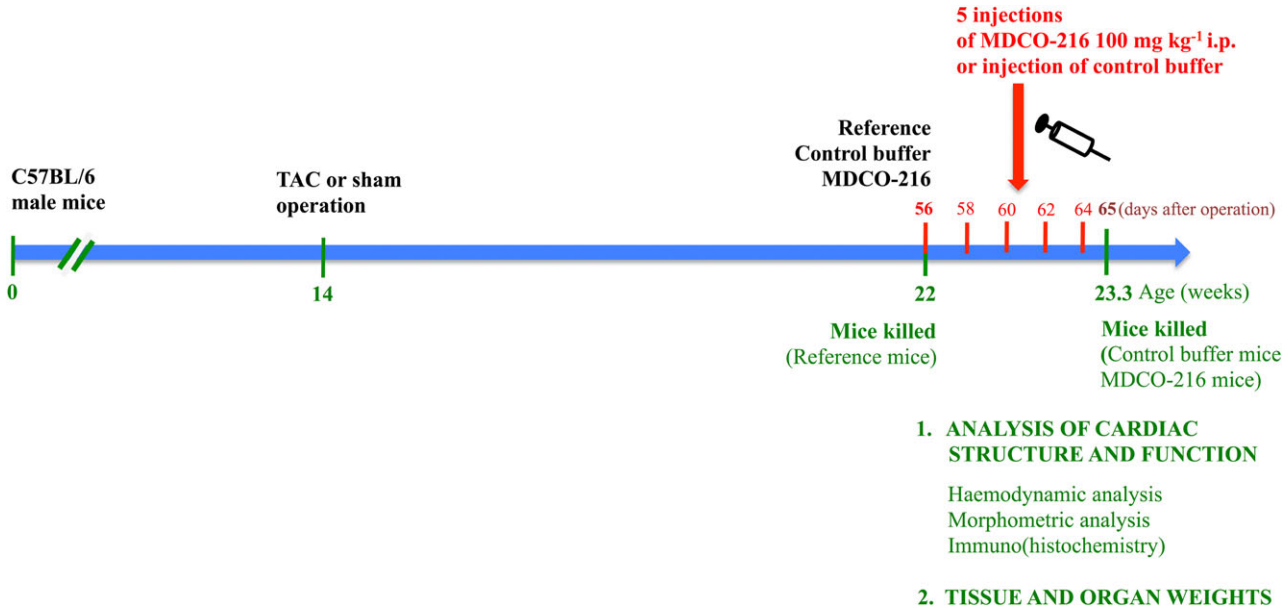

Figure 1
Schematic representation of the study design.

Histological and morphometric analysis

Histological and morphometric analyses were executed as described previously (Muthuramu *et al.,* 2017b). After haemodynamic analysis, mice were perfused *via* the abdominal aorta with PBS and hearts were arrested in diastole by KCl (100 μL; 0.1 mol·L^{-1}), followed by perfusion fixation with 1% paraformaldehyde in PBS. After dissection, hearts were post-fixated overnight in 1% paraformaldehyde, embedded in paraffin, and 6-μm-thick cross sections at 130 μm spaced intervals were made extending from the apex to the basal part of the LV. Comparative sections were subjected to histological and morphometric analyses by using the same slide numbers (1 to 40 from apex to base) and cross-sectional numbers (1–10). LV remodelling was assessed by morphometric analysis on mosaic images of Sirius Red-stained heart cross sections using Axiovision 4.6 software (Zeiss, Zaventem, Belgium). LV wall area and septal wall thickness were determined. All geometric measurements were computed in a blinded fashion from representative tissue sections of four separate regions, and the average value was used to represent that animal for statistical purposes (Van Craeyveld *et al.,* 2012; Gordts *et al.,* 2013).

To measure collagen content in the interstitium, Sirius Red staining was performed as described by Junqueira *et al.* (1979). Sirius Red polarization microscopy on a Leica RBE microscope with KS300 software (Zeiss) was used to quantify thick, tightly packed mature collagen fibres as orange-red birefringent and loosely packed less cross-linked and immature collagen fibres as yellow-green birefringent. Collagen-positive area was normalized to the LV remote area and was expressed as percentage. Any perivascular fibrosis was excluded from this analysis. Perivascular fibrosis was quantified as the ratio of the fibrosis area surrounding the vessel to the total vessel area. Two mid-ventricular sections were studied per animal (Muthuramu *et al.,* 2017b).

Cardiomyocyte hypertrophy was analysed on paraffin sections stained with rabbit anti-mouse laminin (Sigma; 1/50) by measuring the cardiomyocyte cross-sectional area (μm^2) of at least 200 randomly selected cardiomyocytes in the LV myocardium. Capillary density in the myocardium was determined on CD31 stained sections using rat anti-mouse CD31 antibodies (BD; 1/500). Relative vascularity was calculated as the ratio of capillary density to cardiomyocyte density divided by the cardiomyocyte cross-sectional area (Shimizu *et al.,* 2010) and is expressed in μm^{-2}. Two mid-ventricular cross sections were analysed per mouse (Van Craeyveld *et al.,* 2012; Gordts *et al.,* 2013).

Immunostaining for 3-nitrotyrosine was performed with rabbit anti-nitrotyrosine antibodies (Merck Millipore, Overijse, Belgium; dilution 1/250).

Apoptosis was quantified on deparaffinized tissue sections using SignalStain® cleaved caspase-3 IHC detection kit (Cell Signaling Technologies, Beverly, MA, USA), which utilizes a polyclonal rabbit antibody to the neoepitope peptide at the end of cleaved caspase-3 (Muthuramu *et al.,* 2015).

Quantification of plasma lipid levels

Plasma cholesterol levels were determined using a Cholesterol Quantification kit from Sigma (Sigma, St. Louis, MO, USA). HDL and non-HDL lipoproteins were separated by ultracentrifugation as described previously (Muthuramu *et al.,* 2017a). Triglyceride concentration was determined in plasma using the Triglyceride Quantification kit MAK266 (Sigma-Aldrich, Schnelldorf, Germany) according to the instructions of the manufacturer.

Quantification of murine apo A-I

Murine apo A-I plasma levels were determined by ELISA (Mabtech AB, Nacka Strand, Sweden) according to the instructions of the manufacturer. No cross-reaction with wild-type human apo A-I or human apo A-I_{Milano} was observed.

Quantification of myocardial protein levels by Western blot

Myocardial tissue samples were isolated at the time of killing and immediately frozen in liquid nitrogen and stored at −80°C. Tissues were placed in lysing matrix tubes (QBiogene/MP Biomedicals, Solon, OH, USA), mixed with 1 mL of protein extraction buffer containing 10 mM imidazole, 300 mM sucrose, 1 mM dithiotreitol, 1 mM sodium metabisulfite, 25 mM sodium fluoride, 5 mM sodium EDTA, 5 mM sodium pyrophosphate, 0.3 mM PMSF and a protease inhibitor cocktail (Roche Diagnostics Belgium, Vilvoorde, Belgium) (Lenaerts *et al.,* 2013) and homogenized in the FastPrep24 instrument (MP Biomedicals). Protein concentration was quantified using the Pierce BCA Protein Assay kit (Pierce Biotechnology Inc., Rockford, IL, USA). Equal amounts of proteins were separated on 4–20% Tris-Glycine gradient gels (Bio-Rad Laboratories N.V., Temse, Belgium) and blotted onto PVDF membranes (Bio-Rad Laboratories N.V.). Membranes were incubated with primary antibodies against ß-tubulin (Cat# CST 2146), **acetyl-CoA carboxylase** (Cat# CST 3676S) (ACC), p-ACC (Cat# CST 11818S) (Ser^{79}), Smad2/3 (Cat# CST 8685S), Smad4 (Cat# CST 38454S), pyruvate dehydrogenase (Cat# CST 2784) (PDH), **PDH kinase (PDHK)** (Cat# CST 3820), **TGF-β1** (Cat# CST 3711), GAPDH (Cat# CST 2118) (all prior antibodies from Cell Signaling Technologies, Beverly, MA, USA), **PPAR**-α (Cat# ab24509), carnitine palmitoyltransferase IB (CPT1B) (Cat# ab134988), **liver X receptor (LXR)**-α and **LXR-ß** (Cat# ab216691) (Abcam, Cambridge, UK). Protein expression was detected with Super signal west pico chemilumninescent reagents (Thermo Scientific, Rockford, IL, USA) and quantified using Image lab TM Analyser software (Bio-Rad laboratories N.V.). All protein levels were normalized to the GAPDH protein level.

Quantification of myocardial mRNA levels by real-time quantitative reverse transcription PCR

Total RNA was extracted from the LV using RNeasy Mini Kit 74 104 (Qiagen Benelux BV, Antwerp, Belgium). RNA (200 ng) was reverse transcribed into cDNA using the TaqMan™ Reverse Transcription Reagents synthesis kit N8080234 (Fisher Scientific, Brussels, Belgium). Predesigned PrimeTime qPCR probe assays were from Integrated DNA Technologies (Leuven, Belgium) (Supporting Information Table S1). The cDNA amplification reaction was performed using the VeriQuest Probe qPCR Master Mix (2×) 75650 (Life Technologies Europe BV, Merelbeke, Belgium) using a 7500 Fast Real-Time PCR System from Applied Biosystems (Foster City, CA, USA). The 10 μL reaction mixture contained 5 μL

of VeriQuest Probe qPCR Master Mix (2×), 1 μL PrimeTime qPCR probe, 1 μL of cDNA sample and 3 μL of nuclease-free water. A negative control was made using the same volume of nuclease-free water instead of sample. PCR conditions were 50°C for 2 min, 95°C for 10 min followed by 40 cycles of denaturation at 95°C for 15 s and of annealing and extension at 60°C for 40 s. All reactions were done in duplicate to ensure reliability of single values. Normalization of real-time quantitative RT-PCR data was based on multiple internal control genes as originally described by Vandesompele *et al*. (2002). The *Gapdh*, **tubulin alpha 1A (Tuba1a1)** and *eukaryotic translation elongation factor 1 epsilon-1* (*Eef1e1*) were used as internal controls. Relative quantification was performed using the $2^{-\Delta\Delta CT}$ method with reference sham mice providing the reference samples. Normalized mRNA levels were expressed as geometric means ± geometric SE. Therefore, data represent the fold difference versus reference sham mice. The $2^{-\Delta\Delta Ct}$ method was applied to calculate the mRNA levels of **B-cell lymphoma 2 (*Bcl2*)**, Bcl-2-associated X protein (*Bax*), **atrial natriuretic peptide (*Nppa*)**, **brain natriuretic peptide (*Nppb*)**, myosin heavy chain, α isoform (*Myh6*), myosin heavy chain, β isoform (*Myh7*), **collagen, type I, alpha 1 (*Col1a1*)**, **collagen, type III, alpha 1 (*Col3a1*)**, ***Mmp2***, ***Mmp9***, **vascular endothelial growth factor receptor 1(VEGFR-1; *Flt1*)**, **VEGFR-2 (*Kdr*)** and vascular endothelial cadherin (*Cdh5*).

Data and statistical analysis

The data and statistical analysis comply with the recommendations on experimental design and analysis in pharmacology (Curtis *et al.,* 2018). In designing the study, we assumed that survival of TAC mice until day 56, the day of randomization, would be around 60% and that no mortality would occur in sham mice. A second assumption was that haemodynamic measurements would be technically successful in around 70% of TAC mice and in 90% of sham mice.

At the end of the study, data of all surviving mice were included in the analysis. Investigators who performed endpoint analyses were blinded to group allocation. Unblinding of animal numbers corresponding to specific allocation groups was performed at completion of measurements.

Data are expressed as means ± SEM with the exception of normalized mRNA levels that are expressed as geometric means ± geometric SE. Minimally required sample size calculation (n = 14) for haemodynamic analysis in TAC mice was based on a statistical power of 90%, a two-sided cut-off value of statistical significance of 0.05, a difference of main haemodynamic parameters at the population level of 15%, and a SD at population level at 15% of the average of population means. Parameters between the three TAC groups or the three sham groups were compared by one-way ANOVA followed by Tukey's multiple comparisons *post* test for comparing sham groups, TAC groups and sham versus respective TAC groups using GraphPad Instat (GraphPad Software, San Diego, CA, USA). When the assumption of sampling from populations with identical SDs was not met, a logarithmic transformation was performed. When the assumption of sampling from populations with Gaussian distributions was not met, a Kruskal–Wallis test was performed followed by Dunn's multiple comparisons *post* test. Parameters between sham groups and respective TAC groups were compared using Student's *t*-test. When indicated, a logarithmic transformation or a non-parametric Mann–Whitney test was performed. The assumption of Gaussian distribution was tested using the Kolmogorov–Smirnov method. Kaplan–Meier survival curves were analysed by log-rank test using Prism4 (GraphPad Software). A two-sided P value of less than 0.05 was considered statistically significant.

Nomenclature of targets and ligands

Key protein targets and ligands in this article are hyperlinked to corresponding entries in http://www.guidetopharmacology.org, the common portal for data from the IUPHAR/BPS Guide to PHARMACOLOGY (Harding *et al.,* 2018), and are permanently archived in the Concise Guide to PHARMACOLOGY 2017/18 (Alexander *et al.,* 2017a,b,c,d,e).

Results

Survival after TAC

Sham or TAC surgery was performed at the age of 14 weeks. The total number of mice at the start of the sham arm of the study was 65 whereas this number was 143 for the TAC arm of the study. None of the sham mice died whereas survival was 65.0% in the TAC mice before randomization at day 56 after TAC (Figure 2). Following randomization, no additional mice died till day 65 in the control buffer TAC group and the MDCO-216 TAC group.

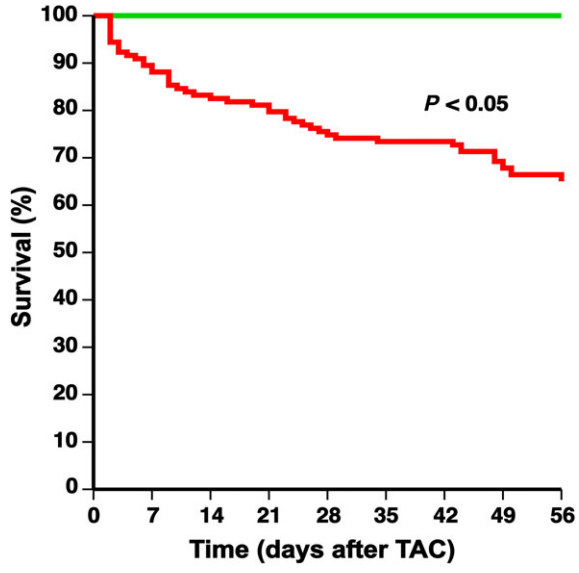

Figure 2

Comparison of Kaplan–Meier survival curves during an 8 weeks follow-up period after TAC or sham operation. C57BL/6 sham mice (green line) and C57BL/6 TAC mice (red line) are compared. The 0 day time-point corresponds to TAC or sham operation at the age of 14 weeks. Survival analysis was performed by log-rank test. The total number of mice at the start of the sham arm of the study was 65 whereas this number was 143 for the TAC arm of the study.

Effect of recombinant HDL$_{Milano}$ on plasma lipid and murine apo A-I levels

Total cholesterol, non-HDL cholesterol, HDL cholesterol and triglyceride plasma levels in C57BL/6 mice at time of killing are shown in Supporting Information Table S2. No major differences were observed. Murine apo A-I levels in MDCO-216-treated mice (337 ± 44 mg·L^{-1}; n = 8) were reduced by 63.7% and by 62.8% compared to reference mice (930 ± 73 mg·L^{-1}; n = 8) and buffer mice (906 ± 60 mg·L^{-1}; n = 8) respectively.

Treatment with recombinant HDL$_{Milano}$ reduces lung weight and atrial weight compared to reference TAC mice

Body weights and organ weights in sham and TAC mice are summarized in Figure 3. No significant difference in body weight was observed between the three sham groups and the three TAC groups and between sham and respective TAC groups (Figure 3A). Heart weight was increased by 1.73-fold, 1.80-fold and 1.67-fold in reference TAC, buffer TAC and MDCO-216 TAC groups, respectively, compared to respective sham groups (Figure 3B). No significant differences of tibia length (Supporting Information Figure S1) were observed between different groups. Consequently, differences of the heart weight/tibia length ratio (Figure 3C) were proportional to differences of heart weight. Similar differences were also observed for left ventricular weight (Figure 3D). Right ventricular weight was 1.39-fold higher in reference TAC mice, 1.30-fold higher in buffer TAC mice and 1.32-fold higher in MDCO-216 TAC mice compared to respective sham groups (Figure 3E). Atrial weight was more than doubled in all TAC groups compared to respective sham groups (Figure 3F). However, atrial weight in MDCO-216 TAC mice was reduced by 19.6% and by 33.0% compared to reference TAC mice and to buffer TAC mice respectively (Figure 3F). Lung weight was 1.45-fold and 1.54-fold higher in reference TAC mice and in control buffer TAC mice, respectively, than in respective sham groups (Figure 3G). In contrast, lung weight was not increased in MDCO-216 TAC mice compared to sham mice. Lung weight in MDCO-216 TAC mice was 25.3% lower than in reference TAC mice and 27.9% lower than in control buffer TAC mice (Figure 3G). No significant differences of liver weight (Figure 3H) were observed between different groups. Taken together, MDCO-216 significantly decreases both atrial weight and lung weight compared to reference TAC mice. These data suggest that MDCO-216 caused a sustained decrease of filling pressures and a reversal of lung oedema.

Treatment with MDCO-216 reduces cardiomyocyte cross-sectional area and increases relative vascularity in the myocardium compared to reference TAC mice

Left ventricular wall area was increased by 1.35-fold, 1.31-fold and 1.36-fold in reference TAC, buffer TAC and MDCO-

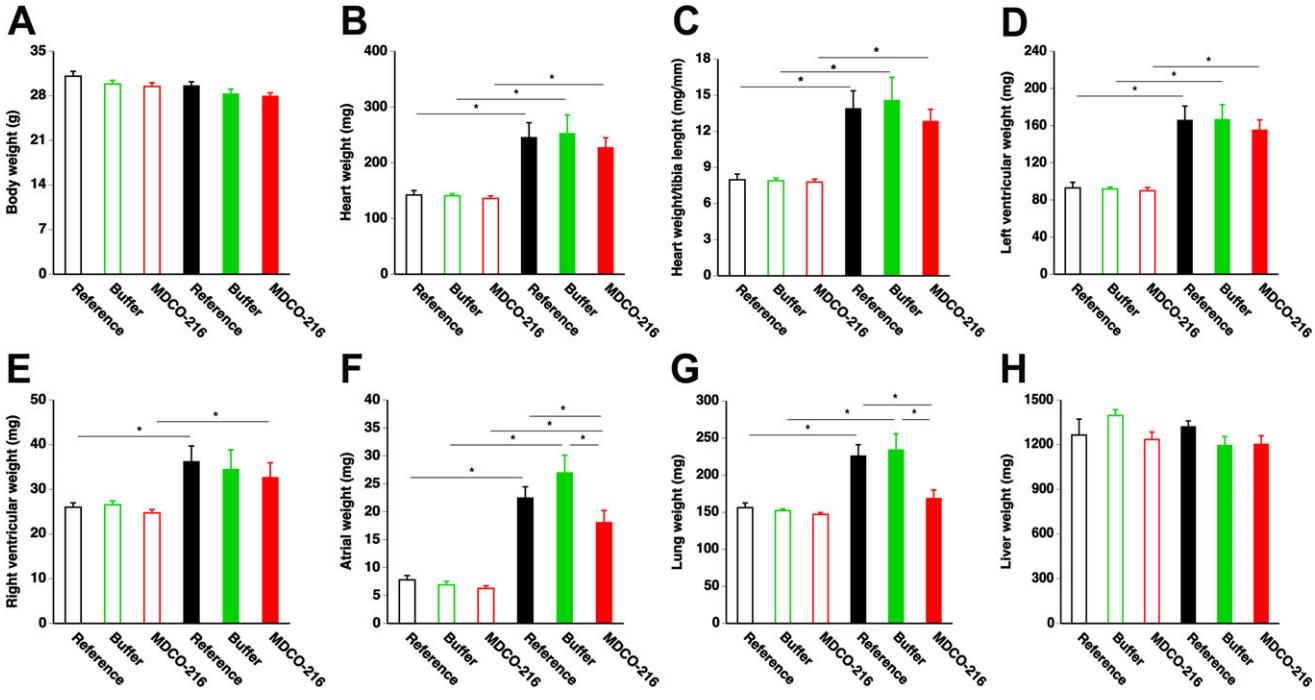

Figure 3

Body weight (A), heart weight (B), heart weight/tibia length (C), left ventricular weight (D), right ventricular weight (E), atrial weight (F), lung weight (G) and liver weight (H) in C57BL/6 sham mice and in C57BL/6 TAC mice. Data reflect wet weights at day 56 (reference mice) and at day 65 (buffer mice and MDCO-216 mice) after sham operation (n = 10 for reference mice, n = 11 for buffer mice, n = 11 for MDCO-216 mice) or TAC (n = 12 for reference mice, n = 12 for buffer mice, n = 10 for MDCO-216 mice). Sham mice and TAC mice are indicated by open and closed bars respectively. All data represent means ± SEM. *P < 0.05.

216 TAC groups, respectively, compared to respective sham groups (Supporting Information Figure S2A). A significant increase of septal wall thickness was also observed after TAC (Supporting Information Figure S2B). Cardiac hypertrophy after TAC is illustrated by representative Sirius Red-stained cross sections of sham hearts and TAC hearts in Supporting Information Figure S2C. Microscopic histological data are illustrated in Figure 4. Cardiomyocyte cross-sectional area was increased in TAC groups compared to respective sham groups (Figure 4A). However, cardiomyocyte cross-sectional area in MDCO-216 TAC mice was significantly reduced by 11.3% and by 10.8% compared to reference TAC mice and control buffer TAC mice respectively (Figure 4A). Cardiomyocyte density (Figure 4B), capillary density (Figure 4C) and relative vascularity (Figure 4D) were significantly lower in TAC groups compared to respective sham groups. Relative vascularity in MDCO-216 TAC mice was increased by 13.9% and by 9.82% compared to reference TAC mice and control buffer TAC mice respectively (Figure 4D). Figure 4E shows representative photomicrographs of laminin-stained cardiomyocytes and CD31-positive capillaries. Taken together, the increase in relative vascularity in the myocardium in MDCO-216 TAC mice compared to reference TAC mice and control buffer TAC mice represents an improvement of the balance between the vascular and cardiomyocyte compartment in the myocardium and may counteract heart failure.

To further corroborate the observed data on heart failure, cardiomyocyte hypertrophy and relative vascularity, mRNA levels of several marker genes were quantified by RT-qPCR (Figure 5). The geometric means of the normalized myocardial mRNA level of atrial natriuretic peptide (*Nppa*) in buffer TAC mice was 2.28-fold higher than in reference TAC mice and 2.28-fold higher than in MDCO-216 TAC mice (Figure 5A). Normalized myocardial mRNA level of brain natriuretic peptide (*Nppb*) in MDCO-216 TAC mice was reduced by 49.7 and 47.1% compared to reference TAC mice and buffer TAC mice respectively (Figure 5B). The geometric means of the normalized myocardial mRNA level of myosin heavy chain, αisoform (*Myh6*) in MDCO-216 TAC mice was 70.0 and 80.7% lower than in reference TAC mice and buffer TAC mice

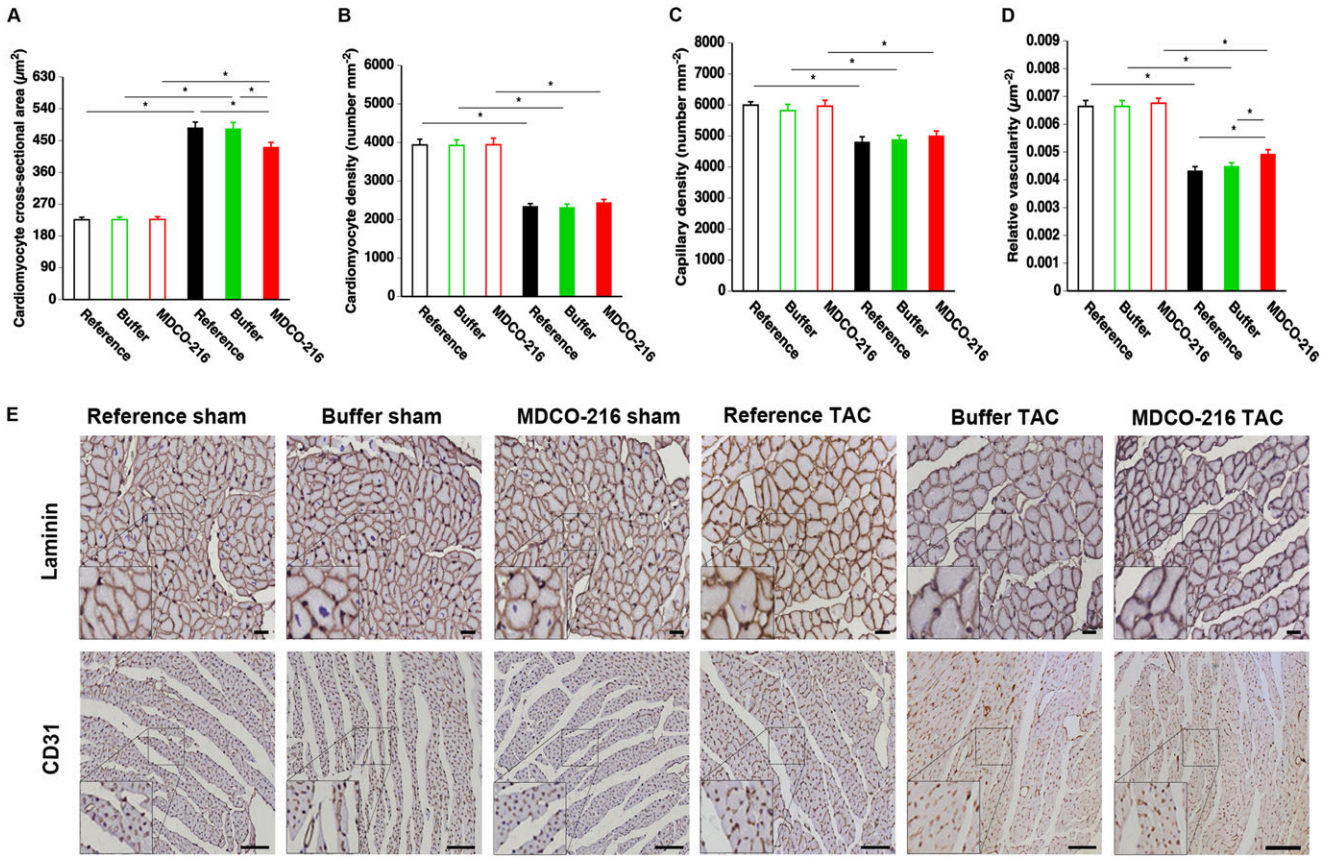

Figure 4

Quantification of immunohistochemical parameters in the myocardium of C57BL/6 sham mice and C57BL/6 TAC mice. Bar graphs showing cardiomyocyte cross-sectional area (A), cardiomyocyte density (B), capillary density (C) and relative vascularity (D) in reference sham mice (n = 11), buffer sham mice (n = 12), MDCO-216 sham mice (n = 10), reference TAC mice (n = 21), buffer TAC mice (n = 17) and MDCO-216 TAC mice (n = 21) at day 56 (reference mice) and at day 65 (buffer mice and MDCO-216 mice) after sham or TAC operation. Sham mice and TAC mice are indicated by open and closed bars respectively. All data represent means ± SEM. *$P < 0.05$. Panel (E) shows representative photomicrographs of laminin-stained cardiomyocytes and CD31-positive capillaries. Scale bar represents 50 μm. Insets show a 4× magnification of the boxed region.

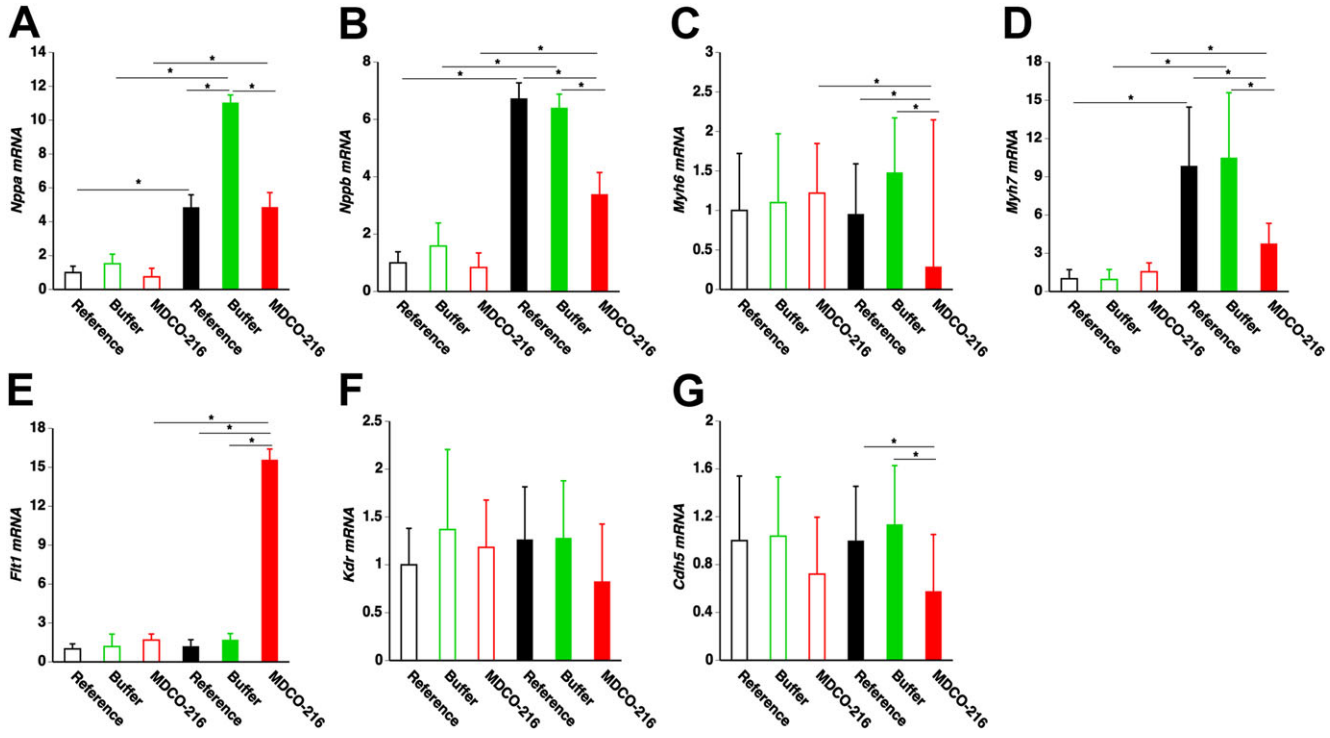

Figure 5

Myocardial mRNA levels of marker genes of heart failure and cardiac remodelling. Bar graphs showing normalized myocardial mRNA levels of *Nppa* (A), *Nppb* (B), *Myh6* (C), *Myh7* (D), *Flt1* (E), *Kdr* (F) and *Cdh5* (G) quantified by RT-qPCR. Data are expressed as geometric means ± geometric SE ($n = 8$). *$P < 0.05$.

respectively (Figure 5C). Similarly, mRNA levels of myosin heavy chain, ß isoform (*Myh7*) in MDCO-216 TAC mice were reduced by 62.0 and 64.3% compared to reference TAC mice and buffer TAC mice respectively (Figure 5D). The normalized myocardial mRNA level of vascular endothelial growth factor receptor 1 (*Flt1*) in MDCO-216 TAC mice was 13.2-fold and 9.26-fold higher than in reference TAC mice and buffer TAC mice respectively (Figure 5E). No significant differences were observed in the normalized myocardial mRNA level of vascular endothelial growth factor receptor 2 (*Kdr*) (Figure 5F). The normalized myocardial mRNA level of vascular endothelial cadherin (*Cdh5*) in MDCO-216 TAC mice was reduced by 42.4 and 49.3% compared to reference TAC mice and buffer TAC mice respectively (Figure 5G).

Reversal of interstitial fibrosis in mice treated with recombinant HDL$_{Milano}$

Pressure overload induced a pronounced increase in myocardial interstitial fibrosis (Figure 6A) and perivascular fibrosis (Figure 6B). Myocardial interstitial fibrosis in MDCO-216 TAC mice was significantly reduced by 32.7% compared to reference TAC mice and by 51.2% compared to control buffer TAC mice. Perivascular fibrosis in MDCO-216 TAC mice was 20.8% lower than in control buffer TAC mice. Figure 6E shows representative photomicrographs of Sirius red-stained interstitial collagen and of perivascular collagen viewed under polarized light.

To evaluate the effect of MDCO-216 on the regression of fibrosis in TAC mice at the molecular level, TGF-β1/Smad signalling in myocardial fibrosis was evaluated by Western blot. The 25-kD isoform of TGF-ß1 (Figure 7A) and Smad2/3 (Figure 7B) were significantly elevated in TAC groups compared to sham groups. Smad4 protein level in MDCO-216 TAC mice was reduced by 19.8 and 22.4% compared to reference TAC mice and buffer TAC mice respectively (Figure 7C). To confirm that the housekeeping protein GAPDH is an adequate reference for normalizing protein expression levels, GAPDH and ß-tubulin expression levels were compared (Figure 7D). GAPDH/ß-tubulin ratios were nearly identical in the six different groups. Representative Western blot images are shown in Figure 7E. The geometric means of the normalized mRNA level of collagen, type I, α 1 (*Col1a1*) in MDCO-216 TAC mice was reduced by 42.6 and 55.0% compared to reference TAC mice and buffer TAC mice respectively (Figure 7F). Normalized mRNA levels of collagen, type III, α 1 (*Col3a1*) were not significantly different between the three TAC groups (Figure 7G). Normalized *Mmp2* mRNA level was significantly lower in MDCO-216 TAC mice compared to the other two TAC groups (Figure 7H). The geometric means of normalized *Mmp9* mRNA level in MDCO-216 TAC mice was 9.41-fold and 6.53-fold higher than in reference TAC mice and buffer TAC mice respectively (Figure 7I). Taken together, MDCO-216 may induce regression of fibrosis in TAC mice by decreased TGF-β1 signalling, decreased *Col1a1* expression and increased *Mmp2* expression.

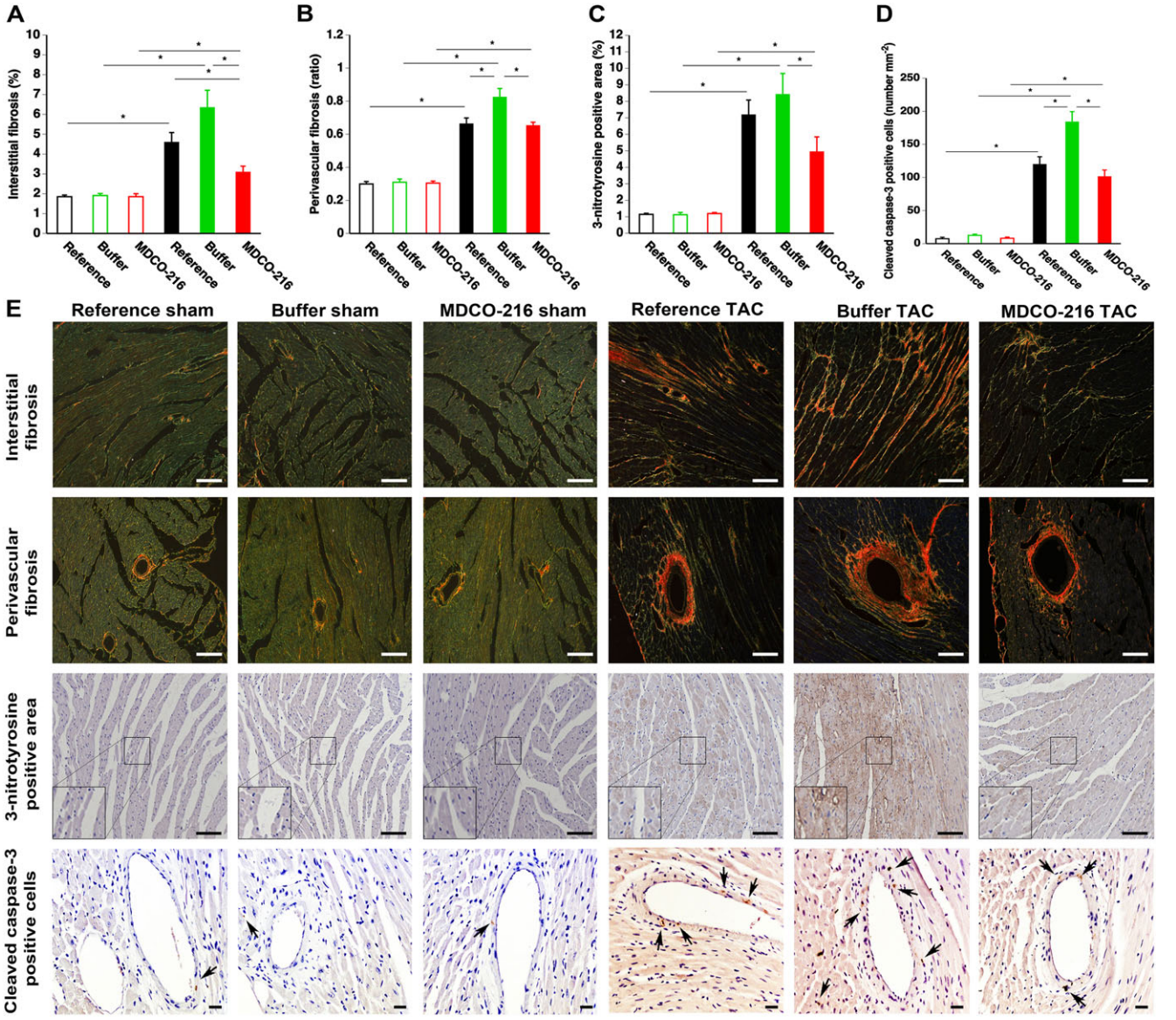

Figure 6

MDCO-216 infusion significantly reduces interstitial fibrosis, perivascular fibrosis, oxidative stress and cleaved caspase-3-positive cells in the myocardium after TAC. Sham mice and TAC mice are indicated by open and closed bars respectively. Bar graphs illustrating the degree of interstitial fibrosis (A), the degree of perivascular fibrosis (B), the percentage of 3-nitrotyrosine-positive area in the myocardium (C) and the cleaved caspase-3-positive cells in the myocardium (D) in reference sham mice ($n = 11$), buffer sham mice ($n = 12$), MDCO-216 sham mice ($n = 10$), reference TAC mice ($n = 21$), buffer TAC mice ($n = 17$) and MDCO-216 TAC mice ($n = 21$) at day 56 (reference mice) and at day 65 (buffer mice and MDCO-216 mice) after sham or TAC operation. All data represent means ± SEM. *$P < 0.05$. Panel (E) shows representative photomicrographs of Sirius red-stained interstitial collagen viewed under polarized light, of perivascular collagen viewed under polarized light, of myocardium immunostained for 3-nitrotyrosine and of myocardium stained for cleaved caspase-3. Scale bar represents 50 μm. Insets show a 4× magnification of the boxed region. Arrows indicate cleaved caspase-3-positive cells.

Effects of MDCO-216 on nitro-oxidative stress and apoptosis in the myocardium

Nitro-oxidative stress was increased several folds following TAC compared to sham mice (Figure 6C). The 3-nitrotyrosine-positive area in the myocardium was reduced by 41.3% in MDCO-216 TAC mice compared to control buffer TAC mice (Figure 6C). Apoptosis in the myocardium was evaluated using immunohistochemical quantification of cleaved caspase-3. Cleaved caspase-3-positive cells were scarce in the myocardium of sham mice (Figure 6D). Compared to control buffer TAC mice, the number of cleaved caspase-3-positive cells was reduced by 44.9% ($P < 0.01$) in MDCO-216 TAC mice (Figure 6D). The normalized myocardial mRNA levels of B-cell lymphoma 2 *(Bcl2)* and Bcl-2-associated X protein *(Bax)* are shown in Supporting Information Figure S3A, B respectively. The myocardial *Bcl2/Bax* mRNA ratio in MDCO-216 TAC mice was 2.83-fold and 2.96-fold higher than in reference TAC mice and in buffer

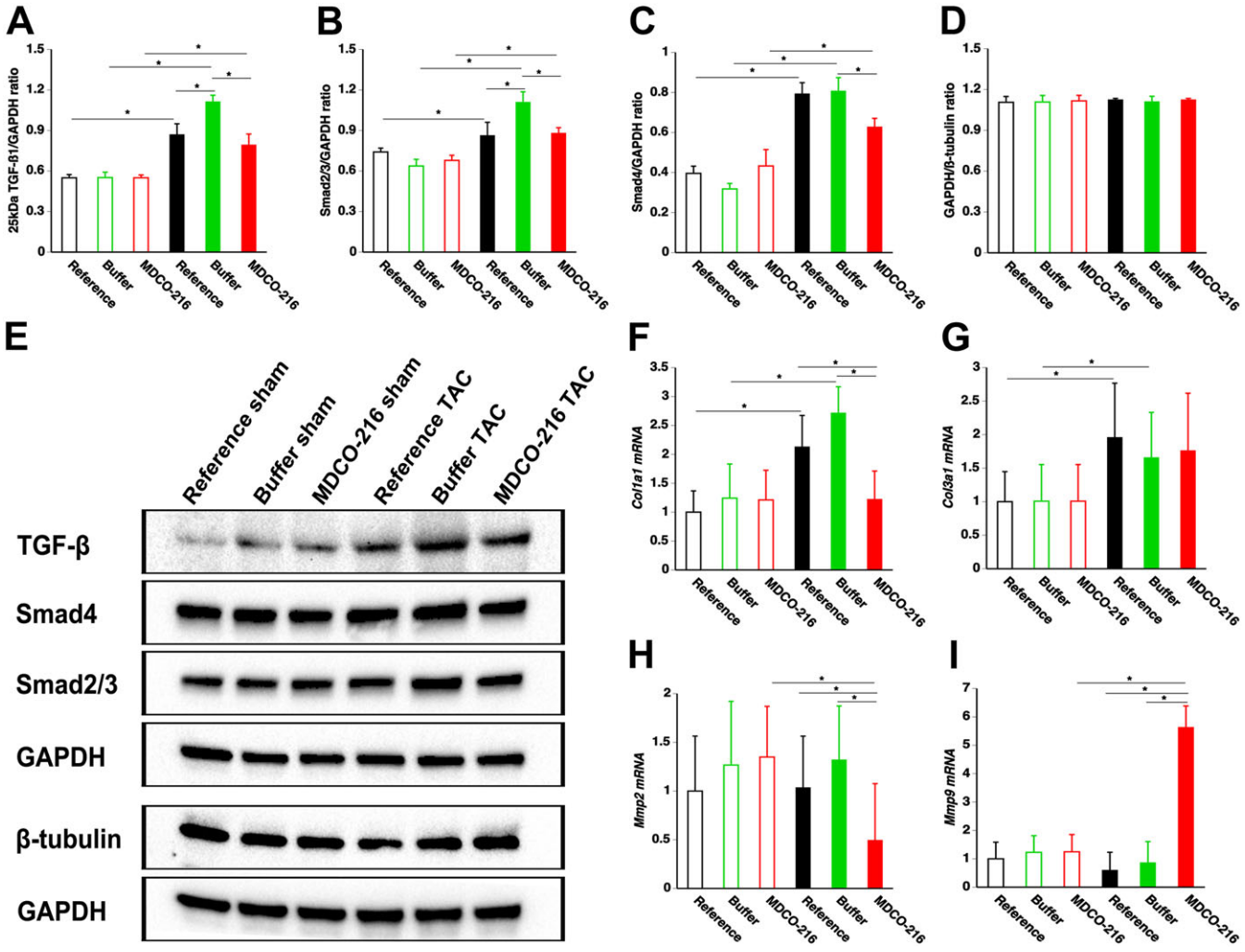

Figure 7

MDCO-216 infusion in TAC mice reduces TGF-β1 signalling, increases *Col1a1* expression and increases *Mmp2* expression in the myocardium. Bar graphs illustrating the 25 kD isoform of TGF-ß1 (A), Smad2/3 (B) and Smad4 (C) myocardial protein levels quantified by Western blot in the myocardium. Sham mice and TAC mice are indicated by open and closed bars respectively. All protein levels were normalized to the GAPDH protein level. The GAPDH/ß-tubulin ratio is shown in panel (D). Representative images of Western blots are shown in panel (E). All data represent means ± SEM ($n = 8$). *$P < 0.05$. Bar graphs showing normalized *Col1a1*, *Col3a1*, *Mmp2* and *Mmp9* mRNA levels quantified by RT-qPCR in the myocardium. Data are expressed as geometric means ± geometric SE ($n = 8$). *$P < 0.05$.

TAC mice respectively (Supporting Information Figure S3C). Figure 6E shows representative photomicrographs of myocardial sections immunostained for 3-nitrotyrosine and for cleaved caspase-3.

Treatment with MDCO-216 improves diastolic function after TAC

Haemodynamic parameters in sham mice and in TAC mice are summarized in Tables 1 and 2 respectively. Systolic and diastolic function was significantly improved in MDCO-216 sham mice compared to control buffer sham mice but not compared to reference sham mice (Table 1). Diastolic function in MDCO-216 TAC mice was significantly improved compared to reference TAC mice and control buffer TAC mice (Table 2). The absolute value of the peak rate of isovolumetric relaxation in MDCO-216 TAC mice was 30.4 and 36.3% higher compared to reference TAC mice and control buffer TAC mice respectively. The time constant of isovolumetric relaxation τ-Glantz in MDCO-216 TAC mice was 10.4% lower than in reference TAC mice and 23.9% lower than in control buffer TAC mice (Table 2). Taken together, treatment with MDCO-216 improves diastolic function after TAC compared to reference TAC mice.

Evaluation of effects of MDCO-216 on cardiac metabolism

To investigate a potential effect of MDCO-216 on myocardial metabolism in TAC mice, key metabolic enzymes, proteins and transcription factors were quantified by Western blot. Protein levels of PDH (Figure 8A) and PDHK (Figure 8B) were not significantly different between sham and TAC mice. Levels of ACC were significantly higher in reference TAC

Table 1

Haemodynamic parameters in C57BL/6 sham mice

	Reference	Buffer	MDCO-216
Number of mice	10	10	10
Left ventricle			
Peak systolic pressure (mmHg)	101 ± 3	96.1 ± 1.7	105 ± 3
End-diastolic pressure (mmHg)	2.84 ± 0.66	2.57 ± 0.45	2.61 ± 0.61
dP/dt_{max} ($mmHg \cdot ms^{-1}$)	12.3 ± 0.6	11.3 ± 0.3	13.5 ± 0.7**
dP/dt_{min} ($mmHg \cdot ms^{-1}$)	−11.8 ± 0.5	−10.2 ± 0.6	−12.8 ± 0.7**
Tau-Weiss (ms)	5.74 ± 0.37	5.70 ± 0.26	4.97 ± 0.24
Tau-Glantz (ms)	6.43 ± 0.36	7.44 ± 0.36	5.61 ± 0.17***
Heart rate (bpm)	613 ± 10	606 ± 15	618 ± 17
Aorta			
Systolic pressure (mmHg)	100 ± 3	96.0 ± 2.8	104 ± 3
Diastolic pressure (mmHg)	59.4 ± 3.2	58.8 ± 3.2	62.3 ± 3.8
Mean pressure (mmHg)	78.8 ± 3.2	76.3 ± 4.0	83.0 ± 3.1

Sham operation was performed in male C57BL/6 mice at the age of 14 weeks. Reference mice were evaluated 8 weeks after sham operation. Five i.p. injections of MDCO-216 (100 $mg \cdot kg^{-1}$) or of an equivalent volume of buffer were performed with a 48 h interval from day 56 till day 64 after operation. Buffer and MDCO-216 mice were investigated at day 65 after operation.

*$P < 0.05$ versus reference.

**$P < 0.05$ versus buffer.

Table 2

Haemodynamic parameters in C57BL/6 TAC mice

	Reference	Buffer	MDCO-216
Number of mice	14	14	20
Left ventricle			
Peak systolic pressure (mmHg)	168 ± 8	163 ± 5	181 ± 5
End-diastolic pressure (mmHg)	4.30 ± 0.93	4.10 ± 0.81	2.17 ± 0.49
dP/dt_{max} ($mmHg \cdot ms^{-1}$)	11.0 ± 0.8	9.52 ± 0.49	11.6 ± 0.2*
dP/dt_{min} ($mmHg \cdot ms^{-1}$)	−9.38 ± 0.66	−8.97 ± 0.64	−12.2 ± 0.5***
Tau-Weiss (ms)	5.79 ± 0.33	7.02 ± 0.32*	5.31 ± 0.18**
Tau-Glantz (ms)	8.52 ± 0.36	10.0 ± 0.5*	7.64 ± 0.21***
Heart rate (bpm)	601 ± 13	615 ± 17	629 ± 11
Aorta			
Systolic pressure (mmHg)	167 ± 10	164 ± 5	178 ± 6
Diastolic pressure (mmHg)	62.7 ± 7.8	61.1 ± 3.0	62.2 ± 2.3
Mean pressure (mmHg)	103 ± 4	100 ± 3	106 ± 3

TAC operation was performed in male C57BL/6 mice at the age of 14 weeks. Reference mice were evaluated 8 weeks after TAC operation. Five i.p. injections of MDCO-216 (100 $mg \cdot kg^{-1}$) or of an equivalent volume of buffer were performed with a 48 h interval from day 56 till day 64 after operation. Buffer and MDCO-216 mice were investigated at day 65 after operation.

*$P < 0.05$ versus reference.

**$P < 0.05$ versus buffer.

mice and buffer TAC mice compared to respective sham groups but were not significantly elevated in MDCO-216 TAC mice (Figure 8C). Levels of p-ACC (Figure 8D), which constitutes the inactive form of the enzyme, were significantly lower in MDCO-216 TAC mice compared to the two other TAC groups. Protein levels of the key metabolic transcriptional factors LXR-α (Figure 8E), LXR-ß (Figure 8F) and PPAR-α (Figure 8G) were not significantly different between sham and TAC groups. Consistently, myocardial protein levels of carnitine palmitoyltransferase IB (CPT1B) were not significantly different between sham and TAC groups. Representative images are shown in panel I. Overall,

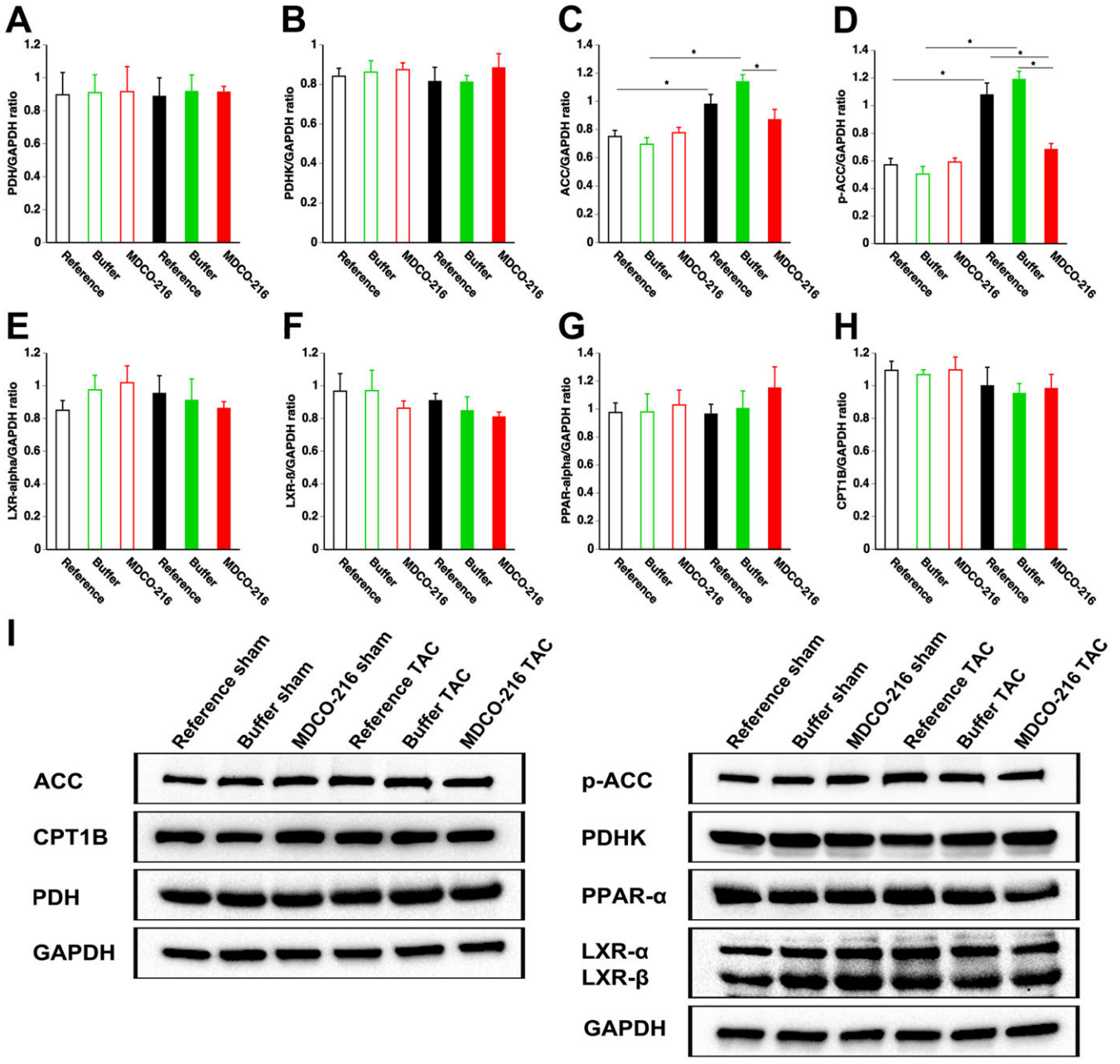

Figure 8

Quantification of metabolic proteins in the myocardium by Western blot. Bar graphs illustrating PDH (A), PDHK (B), AAC (C), p-ACC (D), LXR-α (E), LXR-ß (F), PPAR-α(G) and CPT1B (H) protein levels quantified by Western blot in the myocardium. Sham mice and TAC mice are indicated by open and closed bars respectively. Representative images of Western blots are shown in panel (I). All protein levels were normalized to the GAPDH protein level. All data represent means ± SEM ($n = 8$). *$P < 0.05$.

these results do not directly suggest that there was a major effect of MDCO-216 on substrate metabolism in TAC mice.

Discussion

This murine study evaluating the effect of MDCO-216 demonstrates for the first time that an HDL-targeted intervention reverses pathological remodelling induced by pressure overload and constitutes a successful treatment for heart failure. This reversal in MDCO-216 TAC mice compared to reference TAC mice is highlighted by the increase of relative vascularity and the regression of interstitial fibrosis, by the improved diastolic function, by a decrease of atrial weight and by a normalization of wet lung weight.

MDCO-216 has been administered by intravenous infusion in humans (Kallend *et al.*, 2016; Kempen *et al.*, 2016a; Kempen *et al.*, 2016b). In the current murine study, intraperitoneal administration was applied, which is the most appropriate strategy from a pharmacokinetic point of view since

the effect of intravenous infusion is mimicked (Jung *et al.*, 2014). Administration of MDCO-216 had no effect on HDL cholesterol levels 24 h after the last injection. The lack of an increase of HDL cholesterol may be secondary to the decrease of murine apo A-I levels, which has also previously been observed after apo A-I_{Milano} gene transfer in mice (Feng *et al.*, 2009). In addition, dimeric apo A-I_{Milano} imposes a steric constraint that limits HDL core expansion (Bielicki *et al.*, 1997). Taken together, the effect of MDCO-216 on HDL should be understood in terms of qualitative changes.

Manufactured MDCO-216 particles in solution are small with a diameter determined by non-denaturing polacrylamide gradient gel electrophoresis of 7.8 nm (Kempen *et al.*, 2013). This diameter is consistent with earlier data on reconstituted HDL containing dimeric apo A-I_{Milano} by Calabresi *et al*. (1997). This is clearly smaller than the average size of naturally occurring HDL, which consists of a mixture of particles between 8 and 13 nm in humans and of a monodisperse population with an average diameter of 9.5 nm in mice (Rubin *et al.*, 1991). Previous studies (Kempen *et al.*, 2014; Kempen *et al.*, 2016a) have described *in extenso* rapid remodelling of human HDL following infusion of MDCO-216 in humans or upon addition of MDCO-216 to human serum. In essence, the average HDL diameter transiently increased after infusion due to incorporation of the apo A-I_{Milano} and POPC of MDCO-216. In addition, there was also a rapid and transient increase in pre-ß-HDL, containing free apo A-I displaced from the endogenous HDL and prone to be cleared rapidly from the circulation (Kempen *et al.*, 2014; Kempen *et al.*, 2016a). Presumably, this remodelling also occurs upon intraperitoneal administration of MDCO-216 in mice, as may be inferred from the drop in mouse apo A-I. Polydisperse HDL particles with diameters of 9.7, 8.2 and 7.4 nm have been previously observed after human apo A-I_{Milano} gene transfer in mice (Feng *et al.*, 2009).

The dose of MDCO-216 in this study was based on an initial dose–response evaluation comparing two different doses (100 mg·kg^{-1} protein and 50 mg·kg^{-1} protein). In our dose–response experiments, we did not observe a clear trend for a favourable effect of MDCO-216 on haemodynamic parameters in TAC mice treated with the dose of 50 mg·kg^{-1} protein MDCO-216 (n = 8). Therefore, it was futile to further evaluate this dose taking into account that the assumptions of the statistical power calculation in terms of effect could not be met.

Cardiomyocyte cross-sectional area was reduced in MDCO-216 TAC mice compared to the two other TAC groups, showing for the first time that an HDL-targeted intervention may induce regression of cell hypertrophy. Consistently, treatment with MDCO-216 significantly reduced myocardial mRNA levels of *Nppb*, *Myh6* and *Myh7*. Microvascular rarefaction and compromised myocardial perfusion are typically observed under conditions of structural remodelling of the myocardium induced by overload (Gonzalez *et al.*, 2011). In contrast, physiological hypertrophy involves coordinated tissue growth and angiogenesis (Shiojima *et al.*, 2005). In pathological hypertrophy, mismatch between cardiomyocyte size and vascularity may induce myocardial hypoxia and cardiomyocyte death, which promotes congestive heart failure (Sano *et al.*, 2007). The increase of relative vascularity by MDCO-216 in TAC mice implies an improvement of the balance between the vascular and cardiomyocyte compartment in the myocardium and may result in a better protection against heart failure (Shimizu *et al.*, 2010). Increased *Flt1* expression and an endothelial progenitor cell-mediated effect (Feng *et al.*, 2011) of MDCO-216 on angiogenesis and vasculogenesis may have contributed to the increase of relative vascularity.

Left ventricular pressure overload induced by TAC initially results in reactive interstitial fibrosis and is subsequently succeeded by replacement fibrosis in areas of cardiomyocyte cell death (Travers *et al.*, 2016). One of the salient findings of the current study is the partial reversal of myocardial interstitial fibrosis in MDCO-216 TAC mice. Whereas the zebrafish heart is characterized by endogenous mechanisms of fibrosis regression and by the potential for myocardial regeneration (Gonzalez-Rosa *et al.*, 2011), the potential for regression of myocardial fibrosis in mammalian hearts is likely limited. Reversal of myocardial fibrosis was documented in a TAC model by the combination of aortic debanding and granulocyte colony-stimulating factor treatment (Szardien *et al.*, 2012). In contrast, pressure overload in this study was maintained during the intervention phase. In general, the unique observation of this study is the demonstration of reversal of myocardial fibrosis in the presence of a persistent very high afterload.

HDL has been shown to reduce TGF-ß1-induced collagen deposition in murine fibroblasts (Spillmann *et al.*, 2016). Furthermore, HDL has been demonstrated to decrease TGF-ß1-induced endothelial-mesenchymal transition in aortic endothelial cells *in vitro* (Spillmann *et al.*, 2015). The antifibrotic effects of HDL have been documented in several experimental animal studies. However, these studies documented inhibition of progression of fibrosis and did not investigate reversal of myocardial fibrosis. Adenoviral human *apo A-I* gene therapy reduced oxidative stress, inflammation and myocardial fibrosis in a rat model of diabetic cardiomyopathy (Van Linthout *et al.*, 2008). Recently, we demonstrated that adeno-associated viral serotype 8 human *apo A-I* gene therapy before TAC potently reduced myocardial interstitial fibrosis (Amin *et al.*, 2017). Reconstituted HDL decreases total collagen content in aortic valves in a murine model of aortic stenosis in comparison with a placebo progression group (Trapeaux *et al.*, 2013).

Intervention with MDCO-216 improved diastolic function in both sham mice and in TAC mice. This finding is consistent with previous observations on the effect of gene therapy with an E1E3E4-deleted human *apo A-I* vector in C57BL/6 LDL receptor-deficient mice (Gordts *et al.*, 2012) and in diabetic mice (Van Linthout *et al.*, 2008). Improved diastolic function has also been observed after gene therapy with an adeno-associated viral serotype 8 human *apo A-I* vector in C57BL/6 LDL receptor-deficient mice (Amin *et al.*, 2017). In a model of cholesterol- and vitamin D2-enriched diet-induced mild aortic valve stenosis and left ventricular hypertrophy in rabbits, the HDL mimetic peptide CER-522 improved echocardiographic indices of left ventricular diastolic dysfunction (Merlet *et al.*, 2016).

An operational definition of heart failure in mice can be based on the presence of increased wet lung weight

indicating pulmonary congestion. The critical finding in the current study is that MDCO-216 reversed increased lung weight compared to reference TAC mice. The decrease of atrial weight and of myocardial *Nppb* mRNA levels in MDCO-216 TAC mice compared to reference TAC mice suggests a chronic decrease of filling pressures. Taken together, heart failure is reversed by MDCO-216 treatment notwithstanding continued increased afterload.

A limitation of the current study is that we did not evaluate for how long the beneficial effects of MDCO-216 on cardiac function and on cardiac structure persist in mice with pressure overload. Furthermore, the study was restricted to male mice. It remains to be established that the effect of MDCO-216 is of similar magnitude in female mice. Significant sex differences in the degree of left ventricular hypertrophy after TAC exist (Witt *et al.,* 2008; Kararigas *et al.,* 2014) and sex differences in heart failure incidence and prognosis in humans should be considered in the further preclinical development of HDL-targeted therapies for heart failure. Moreover, since heart failure with preserved ejection fraction represents a major unmet therapeutic need, the efficacy of MDCO-216 should also be demonstrated in models of heart failure with preserved ejection fraction.

In conclusion, MDCO-216 improves diastolic function, induces regression of interstitial fibrosis, decreases atrial weight and normalizes lung weight in mice with established heart failure. Recombinant HDL may emerge as a treatment modality for heart failure.

Acknowledgements

I.M. is a postdoctoral fellow of the Fonds voor Wetenschappelijk Onderzoek-Vlaanderen. This work was supported by Onderzoekstoelagen grant OT/13/090 of the KU Leuven and by grant G0A3114N of the Fonds voor Wetenschappelijk Onderzoek-Vlaanderen.

Author contributions

B.D.G. and H.K. conceived and designed the experiments; J.P.A., M.M., R.A. and I.M. performed the experiments; J.P.A., M.M., R.A., I.M. and B.D.G. analysed the data; J.P.A., M.M., R.A. and B.D.G. wrote the paper; and B.D.G was responsible for funding acquisition.

Conflict of interest

The authors declare no conflicts of interest.

Dr Herman Kempen was an employee of The Medicines Company (Schweiz) GmbH between 2011 and 2015 and retired subsequently. He does not benefit in any financial manner from being co-author on this paper. None of the other authors received any financial support of The Medicines Company.

Declaration of transparency and scientific rigour

This Declaration acknowledges that this paper adheres to the principles for transparent reporting and scientific rigour of preclinical research recommended by funding agencies, publishers and other organisations engaged with supporting research.

References

Alexander SP, Christopoulos A, Davenport AP, Kelly E, Marrion NV, Peters JA *et al.* (2017a). The Concise Guide to PHARMACOLOGY 2017/18: G protein-coupled receptors. Br J Pharmacol 174: S17–S129.

Alexander SP, Cidlowski JA, Kelly E, Marrion NV, Peters JA, Faccenda E *et al.* (2017b). The Concise Guide to PHARMACOLOGY 2017/18: nuclear hormone receptors. Br J Pharmacol 174: S208–S224.

Alexander SP, Fabbro D, Kelly E, Marrion NV, Peters JA, Faccenda E *et al.* (2017c). The Concise Guide to PHARMACOLOGY 2017/18: catalytic receptors. Br J Pharmacol 174: S225–S271.

Alexander SP, Fabbro D, Kelly E, Marrion NV, Peters JA, Faccenda E *et al.* (2017d). The Concise Guide to PHARMACOLOGY 2017/18: enzymes. Br J Pharmacol 174: S272–S359.

Alexander SP, Kelly E, Marrion NV, Peters JA, Faccenda E, Harding SD *et al.* (2017e). The Concise Guide to PHARMACOLOGY 2017/18: overview. Br J Pharmacol 174: S1–S16.

Amin R, Muthuramu I, Aboumsallem JP, Mishra M, Jacobs F, De Geest B (2017). Selective HDL-raising human Apo A-I gene therapy counteracts cardiac hypertrophy, reduces myocardial fibrosis, and improves cardiac function in mice with chronic pressure overload. Int J Mol Sci 18: 1–14.

Bielicki JK, Forte TM, McCall MR, Stoltzfus LJ, Chiesa G, Sirtori CR *et al.* (1997). High density lipoprotein particle size restriction in apolipoprotein A-I (Milano) transgenic mice. J Lipid Res 38: 2314–2321.

Calabresi L, Vecchio G, Frigerio F, Vavassori L, Sirtori CR, Franceschini G (1997). Reconstituted high-density lipoproteins with a disulfide-linked apolipoprotein A-I dimer: evidence for restricted particle size heterogeneity. Biochemistry 36: 12428–12433.

Curtis MJ, Alexander S, Cirino G, Docherty JR, George CH, Giembycz MA *et al.* (2018). Experimental design and analysis and their reporting II: updated and simplified guidance for authors and peer reviewers. Br J Pharmacol 175: 987–993.

Feng Y, Gordts SC, Chen F, Hu Y, Van Craeyveld E, Jacobs F *et al.* (2011). Topical HDL administration reduces vein graft atherosclerosis in apo E deficient mice. Atherosclerosis 214: 271–278.

Feng Y, Van Craeyveld E, Jacobs F, Lievens J, Snoeys J, De Geest B (2009). Wild-type apo A-I and apo A-I (Milano) gene transfer reduce native and transplant arteriosclerosis to a similar extent. J Mol Med 87: 287–297.

Franceschini G, Sirtori CR, Capurso A 2nd, Weisgraber KH, Mahley RW (1980). A-IMilano apoprotein. Decreased high density lipoprotein cholesterol levels with significant lipoprotein modifications and without clinical atherosclerosis in an Italian family. J Clin Invest 66: 892–900.

Gonzalez A, Ravassa S, Beaumont J, Lopez B, Diez J (2011). New targets to treat the structural remodeling of the myocardium. J Am Coll Cardiol 58: 1833–1843.

Gonzalez-Rosa JM, Martin V, Peralta M, Torres M, Mercader N (2011). Extensive scar formation and regression during heart regeneration after cryoinjury in zebrafish. Development 138: 1663–1674.

Gordts SC, Muthuramu I, Nefyodova E, Jacobs F, Van Craeyveld E, De Geest B (2013). Beneficial effects of selective HDL-raising gene transfer on survival, cardiac remodelling and cardiac function after myocardial infarction in mice. Gene Ther 20: 1053–1061.

Gordts SC, Singh N, Muthuramu I, De Geest B (2014). Pleiotropic effects of HDL: towards new therapeutic areas for HDL-targeted interventions. Curr Mol Med 14: 481–503.

Gordts SC, Van Craeyveld E, Muthuramu I, Singh N, Jacobs F, De Geest B (2012). Lipid lowering and HDL raising gene transfer increase endothelial progenitor cells, enhance myocardial vascularity, and improve diastolic function. PLoS One 7: e46849.

Gualandri V, Franceschini G, Sirtori CR, Gianfranceschi G, Orsini GB, Cerrone A *et al*. (1985). AIMilano apoprotein identification of the complete kindred and evidence of a dominant genetic transmission. Am J Hum Genet 37: 1083–1097.

Harding SD, Sharman JL, Faccenda E, Southan C, Pawson AJ, Ireland S *et al*. (2018). The IUPHAR/BPS Guide to PHARMACOLOGY in 2018: updates and expansion to encompass the new guide to IMMUNOPHARMACOLOGY. Nucl Acids Res 46: D1091–D1106.

Iwaoka M, Obata JE, Abe M, Nakamura T, Kitta Y, Kodama Y *et al*. (2007). Association of low serum levels of apolipoprotein A-I with adverse outcomes in patients with nonischemic heart failure. J Card Fail 13: 247–253.

Jung C, Kaul MG, Bruns OT, Ducic T, Freund B, Heine M *et al*. (2014). Intraperitoneal injection improves the uptake of nanoparticle-labeled high-density lipoprotein to atherosclerotic plaques compared with intravenous injection: a multimodal imaging study in ApoE knockout mice. Circ Cardiovasc Imaging 7: 303–311.

Junqueira LC, Bignolas G, Brentani RR (1979). Picrosirius staining plus polarization microscopy, a specific method for collagen detection in tissue sections. Histochem J 11: 447–455.

Kallend DG, Reijers JA, Bellibas SE, Bobillier A, Kempen H, Burggraaf J *et al*. (2016). A single infusion of MDCO-216 (ApoA-1 Milano/POPC) increases ABCA1-mediated cholesterol efflux and pre-beta 1 HDL in healthy volunteers and patients with stable coronary artery disease. Eur Heart J Cardiovasc Pharmacother 2: 23–29.

Kararigas G, Fliegner D, Forler S, Klein O, Schubert C, Gustafsson JA *et al*. (2014). Comparative proteomic analysis reveals sex and estrogen receptor beta effects in the pressure overloaded heart. J Proteome Res 13: 5829–5836.

Kempen HJ, Asztalos BF, Moerland M, Jeyarajah E, Otvos J, Kallend DG *et al*. (2016a). High-density lipoprotein subfractions and cholesterol efflux capacities after infusion of MDCO-216 (apolipoprotein A-IMilano/palmitoyl-oleoyl-phosphatidylcholine) in healthy volunteers and stable coronary artery disease patients. Arterioscler Thromb Vasc Biol 36: 736–742.

Kempen HJ, Gomaraschi M, Bellibas SE, Plassmann S, Zerler B, Collins HL *et al*. (2013). Effect of repeated apoA-IMilano/POPC infusion on lipids, (apo) lipoproteins, and serum cholesterol efflux capacity in cynomolgus monkeys. J Lipid Res 54: 2341–2353.

Kempen HJ, Gomaraschi M, Simonelli S, Calabresi L, Moerland M, Otvos J *et al*. (2016b). Persistent changes in lipoprotein lipids after a single infusion of ascending doses of MDCO-216 (apoA-IMilano/POPC) in healthy volunteers and stable coronary artery disease patients. Atherosclerosis 255: 17–24.

Kempen HJ, Schranz DB, Asztalos BF, Otvos J, Jeyarajah E, Drazul-Schrader D *et al*. (2014). Incubation of MDCO-216 (ApoA-IMilano/POPC) with human serum potentiates ABCA1-mediated cholesterol efflux capacity, generates new prebeta-1 HDL, and causes an increase in HDL size. J Lipids 2014: 923903.

Kilkenny C, Browne W, Cuthill IC, Emerson M, Altman DG (2010). Animal research: reporting in vivo experiments: the ARRIVE guidelines. Br J Pharmacol 160: 1577–1579.

Lenaerts I, Driesen RB, Hermida N, Holemans P, Heidbuchel H, Janssens S *et al*. (2013). Role of nitric oxide and oxidative stress in a sheep model of persistent atrial fibrillation. Europace 15: 754–760.

Lin L, Gong H, Ge J, Jiang G, Zhou N, Li L *et al*. (2011). High density lipoprotein downregulates angiotensin II type 1 receptor and inhibits angiotensin II-induced cardiac hypertrophy. Biochem Biophys Res Commun 404: 28–33.

Lin L, Liu X, Xu J, Weng L, Ren J, Ge J *et al*. (2015). High-density lipoprotein inhibits mechanical stress-induced cardiomyocyte autophagy and cardiac hypertrophy through angiotensin II type 1 receptor-mediated PI3K/Akt pathway. J Cell Mol Med 19: 1929–1938.

Luscher TF (2015). Heart failure: the cardiovascular epidemic of the 21st century. Eur Heart J 36: 395–397.

McGrath JC, Lilley E (2015). Implementing guidelines on reporting research using animals (ARRIVE etc.): new requirements for publication in BJP. Br J Pharmacol 172: 3189–3193.

Mehra MR, Uber PA, Lavie CJ, Milani RV, Park MH, Ventura HO (2009). High-density lipoprotein cholesterol levels and prognosis in advanced heart failure. J Heart Lung Transplant 28: 876–880.

Merlet N, Busseuil D, Mihalache-Avram T, Mecteau M, Shi Y, Nachar W *et al*. (2016). HDL mimetic peptide CER-522 treatment regresses left ventricular diastolic dysfunction in cholesterol-fed rabbits. Int J Cardiol 215: 364–371.

Muthuramu I, Amin R, De Geest B (2017). New perspectives on biological HDL-targeted therapies. Expert Opin Biol Ther 17: 793–796.

Muthuramu I, Amin R, Postnov A, Mishra M, Aboumsallem JP, Dresselaers T *et al*. (2017a). Cholesterol-lowering gene therapy counteracts the development of non-ischemic cardiomyopathy in mice. Mol Ther 25: 2513–2525.

Muthuramu I, Amin R, Postnov A, Mishra M, Jacobs F, Gheysens O *et al*. (2017b). Coconut oil aggravates pressure overload-induced cardiomyopathy without inducing obesity, systemic insulin resistance, or cardiac steatosis. Int J Mol Sci 18: 1565.

Muthuramu I, Singh N, Amin R, Nefyodova E, Debasse M, Van Horenbeeck I *et al*. (2015). Selective homocysteine-lowering gene transfer attenuates pressure overload-induced cardiomyopathy via reduced oxidative stress. J Mol Med (Berl) 93: 609–618.

Qin W, Du N, Zhang L, Wu X, Hu Y, Li X *et al*. (2015). Genistein alleviates pressure overload-induced cardiac dysfunction and interstitial fibrosis in mice. Br J Pharmacol 172: 5559–5572.

Reijers JAA, Kallend DG, Malone KE, Jukema JW, Wijngaard PLJ, Burggraaf J *et al*. (2017). MDCO-216 does not induce adverse immunostimulation, in contrast to its predecessor ETC-216. Cardiovasc Drugs Ther 31: 381–389.

Rubin EM, Ishida BY, Clift SM, Krauss RM (1991). Expression of human apolipoprotein A-I in transgenic mice results in reduced plasma levels of murine apolipoprotein A-I and the appearance of two

new high density lipoprotein size subclasses. Proc Natl Acad Sci U S A 88: 434–438.

Sano M, Minamino T, Toko H, Miyauchi H, Orimo M, Qin Y *et al*. (2007). p53-induced inhibition of Hif-1 causes cardiac dysfunction during pressure overload. Nature 446: 444–448.

Shah AS, Tan L, Lu Long J, Davidson WS (2013). The proteomic diversity of high density lipoproteins: our emerging understanding of its importance in lipid transport and beyond. J Lipid Res 54: 2575–2585.

Shimizu I, Minamino T, Toko H, Okada S, Ikeda H, Yasuda N *et al*. (2010). Excessive cardiac insulin signaling exacerbates systolic dysfunction induced by pressure overload in rodents. J Clin Invest 120: 1506–1514.

Shiojima I, Sato K, Izumiya Y, Schiekofer S, Ito M, Liao R *et al*. (2005). Disruption of coordinated cardiac hypertrophy and angiogenesis contributes to the transition to heart failure. J Clin Invest 115: 2108–2118.

Sirtori CR, Calabresi L, Franceschini G, Baldassarre D, Amato M, Johansson J *et al*. (2001). Cardiovascular status of carriers of the apolipoprotein A-I (Milano) mutant: the Limone sul Garda study. Circulation 103: 1949–1954.

Spillmann F, De Geest B, Muthuramu I, Amin R, Miteva K, Pieske B *et al*. (2016). Apolipoprotein A-I gene transfer exerts immunomodulatory effects and reduces vascular inflammation and fibrosis in ob/ob mice. J Inflamm (Lond) 13: 25.

Spillmann F, Miteva K, Pieske B, Tschope C, Van Linthout S (2015). High-density lipoproteins reduce endothelial-to-mesenchymal transition. Arterioscler Thromb Vasc Biol 35: 1774–1777.

Szardien S, Nef HM, Voss S, Troidl C, Liebetrau C, Hoffmann J *et al*. (2012). Regression of cardiac hypertrophy by granulocyte colony-stimulating factor-stimulated interleukin-1beta synthesis. Eur Heart J 33: 595–605.

Trapeaux J, Busseuil D, Shi Y, Nobari S, Shustik D, Mecteau M *et al*. (2013). Improvement of aortic valve stenosis by ApoA-I mimetic therapy is associated with decreased aortic root and valve remodelling in mice. Br J Pharmacol 169: 1587–1599.

Travers JG, Kamal FA, Robbins J, Yutzey KE, Blaxall BC (2016). Cardiac fibrosis: the fibroblast awakens. Circ Res 118: 1021–1040.

Van Craeyveld E, Jacobs F, Gordts SC, De Geest B (2012). Low-density lipoprotein receptor gene transfer in hypercholesterolemic mice improves cardiac function after myocardial infarction. Gene Ther 19: 860–871.

Van Linthout S, Frias M, Singh N, De Geest B (2015). Therapeutic potential of HDL in cardioprotection and tissue repair. Handb Exp Pharmacol 224: 527–565.

Van Linthout S, Spillmann F, Lorenz M, Meloni M, Jacobs F, Egorova M *et al*. (2009). Vascular-protective effects of high-density lipoprotein include the downregulation of the angiotensin II type 1 receptor. Hypertension 53: 682–687.

Van Linthout S, Spillmann F, Riad A, Trimpert C, Lievens J, Meloni M *et al*. (2008). Human apolipoprotein A-I gene transfer reduces the development of experimental diabetic cardiomyopathy. Circulation 117: 1563–1573.

Vandesompele J, De Preter K, Pattyn F, Poppe B, Van Roy N, De Paepe A *et al*. (2002). Accurate normalization of real-time quantitative RT-PCR data by geometric averaging of multiple internal control genes. Genome Biol 3 RESEARCH0034.

Velagaleti RS, Massaro J, Vasan RS, Robins SJ, Kannel WB, Levy D (2009). Relations of lipid concentrations to heart failure incidence: the Framingham Heart Study. Circulation 120: 2345–2351.

Weisgraber KH, Bersot TP, Mahley RW, Franceschini G, Sirtori CR (1980). A-Imilano apoprotein. Isolation and characterization of a cysteine-containing variant of the A-I apoprotein from human high density lipoproteins. J Clin Invest 66: 901–907.

Witt H, Schubert C, Jaekel J, Fliegner D, Penkalla A, Tiemann K *et al*. (2008). Sex-specific pathways in early cardiac response to pressure overload in mice. J Mol Med (Berl) 86: 1013–1024.

Supporting Information

Additional supporting information may be found online in the Supporting Information section at the end of the article.

https://doi.org/10.1111/bph.14463

Figure S1 Tibia length in C57BL/6 sham mice and in C57BL/6 TAC mice. Data reflect measurements at day 56 (reference mice) and at day 65 (buffer mice and MDCO-216 mice) after sham operation (n = 10 for reference mice, n = 11 for buffer mice, n = 11 for MDCO-216 mice) or TAC (n = 12 for reference mice, n = 12 for buffer mice, n = 10 for MDCO-216 mice). Sham mice and TAC mice are indicated by open bars and closed bars respectively.

Figure S2 TAC induces left ventricular hypertrophy. Bar graphs showing the left ventricular wall area (A) and septal wall thickness (B) in reference sham mice (n = 11), buffer sham mice (n = 12), MDCO-216 sham mice (n = 10), reference TAC mice (n = 21), buffer TAC mice (n = 17), and MDCO-216 TAC mice (n = 21) at day 56 (reference mice) and at day 65 (buffer mice and MDCO-216 mice) after sham or TAC operation. Sham mice and TAC mice are indicated by open bars and closed bars, respectively. All data represent means ± SEM. *: $P < 0.05$. Panel C shows representative Sirius red-stained cross-sections of sham hearts and TAC hearts. Scale bar represents 1 mm.

Figure S3 Myocardial mRNA levels of apoptotic markers. Bar graphs showing normalized myocardial mRNA levels of *Bcl2* (A) and *Bax* (B) quantified by RT-qPCR. The *Bcl2 mRNA/Bax* mRNA ratio is shown in panel C. Data are expressed as geometric means ± geometric standard error (n = 8). *: $P < 0.05$.

Table S1 Primers and probe sequences for real-time quantitative reverse transcription PCR.

Table S2 Total, non-HDL, HDL cholesterol, and triglyceride plasma levels in C57BL/6 mice at time of kill.